The Journal of Chemical Physics

Ion condensation behavior and dynamics of water molecules surrounding the sodium poly(methacrylic acid) chain in water: A molecular dynamics study

Yung-Ting Chung and Ching-I Huang

Citation: J. Chem. Phys. **136**, 124903 (2012); doi: 10.1063/1.3697477
View online: http://dx.doi.org/10.1063/1.3697477
View Table of Contents: http://jcp.aip.org/resource/1/JCPSA6/v136/i12
Published by the American Institute of Physics.

Additional information on J. Chem. Phys.

Journal Homepage: http://jcp.aip.org/
Journal Information: http://jcp.aip.org/about/about_the_journal
Top downloads: http://jcp.aip.org/features/most_downloaded
Information for Authors: http://jcp.aip.org/authors

ADVERTISEMENT

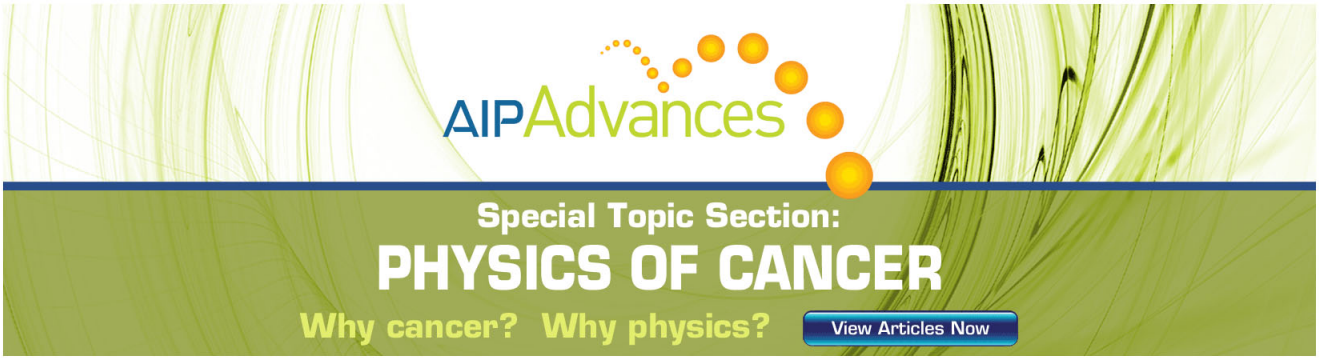

Downloaded 23 Apr 2012 to 140.112.148.95. Redistribution subject to AIP license or copyright; see http://jcp.aip.org/about/rights_and_permissions

Ion condensation behavior and dynamics of water molecules surrounding the sodium poly(methacrylic acid) chain in water: A molecular dynamics study

Yung-Ting Chung and Ching-I Huang[a)]
Institute of Polymer Science and Engineering, National Taiwan University, Taipei 10617, Taiwan

(Received 23 November 2011; accepted 5 March 2012; published online 27 March 2012)

All-atom molecular dynamics simulations are used to study the condensation behavior of monovalent (Na^+) and multivalent (Ca^{2+}) salt counterions associated with the co-ions (Cl^-) surrounding the charged poly(methacrylic acid) (PMAA) chain in water. The study is extended to the influences on chain conformation, local arrangement, and dynamics of water in the highly diluted aqueous solutions. We find that even when the salt ions are monovalent, they attract more than one charged monomer and act as a bridging agent within the chain, as the multivalent salt ions. In principle, the salt ions bridge between not only the "non-adjacent" but also the "adjacent" charged monomers, leading to a more coil-like and a locally stretched conformation, respectively. With an increase in the salt concentration, the amount of coiled-type condensed ions increase and reach a maximum when the chain conformation becomes the most collapsed; whereas, the stretched-type shows an opposite trend. Our results show that the attractive interactions through the condensed salt ions between the non-adjacent monomers are responsible for the conformational collapse. When the salt concentration increases high enough, a significant increase for the stretched-type condensed ions makes an expansion effect on the chain. These stretched-type salt ions, followed by the adsorption of the co-ions and water molecules, tend to form a multilayer organization outside surrounding the PMAA chain. Thus, the expansion degree of the chain conformation is greatly limited. When only the monovalent Na^+ ions are present in the solutions, water molecules are primarily adsorbed into either the condensed Na^+ ions or the COO^- groups. These adsorbed water molecules form hydrogen bonds with each other and enhance the local bridging behavior associated with the Na^+ condensation on the resultant chain conformation. With an increase in the amount of multivalent Ca^{2+} salt ions, more water molecules are bonded directly with the condensed Ca^{2+} ions. In this case, only the condensed Ca^{2+} ions provide a strong bridging effect within the polymer chain. We observe a significant shift towards a higher frequency of the oxygen vibration spectrum and only a slight shift towards a higher frequency of the hydrogen spectrum for the water molecules associated with the ion condensation.
© *2012 American Institute of Physics*. [http://dx.doi.org/10.1063/1.3697477]

I. INTRODUCTION

Polyelectrolytes are macromolecules that contain ionizable groups. They have attracted great interest because of their extensive presence in the biological systems and in a wide range of applications, such as in cosmetics, pharmaceutics, sensors, semiconducting films, biomedical technology, and polymer technology.[1] In these applications, understanding the molecular conformation behavior of polyelectrolytes is a fundamental and important issue, as it plays a crucial role in their performances. Moreover, the presence of salt counterions has significant effects on the structure and dynamics of the polyelectrolyte solutions.

In general, polyelectrolytes dissociate into polyions and counterions in a polar solution. The associated electrostatic interactions make the chain conformation behavior of polyelectrolytes quite distinct from that of neutral polymers. Experiments have shown that polyelectrolyte conformation in dilute solutions depends on the charge density along the chain, the solution *p*H value, the ionic strength, and the added salt concentration.[2–15] For instance, highly charged polyelectrolyte chains at low ionic strength monovalent salt solutions exhibit a stretched (rod-like or coil-like, depending on the salt concentrations) conformation. When the added salts are multivalent, a series of transitions first from stretched to collapsed and then to reexpanded (redissolved) conformations often occurs upon increasing the salts concentrations. Recently, Roiter *et al.* used the *in situ* atomic force microscopy to investigate the single molecule conformation of the highly charged poly(2-vinylpyridine) chains on atomically flat mica in aqueous solutions of NaCl/HCl and Na_2SO_4/H_2SO_4.[15] Even in the presence of monovalent anions, they observed a transition from extended to coil-like and to expanded conformation with an increase in the anion concentration.

Various theoretical models have predicted that the attractive interactions via the associated condensation from multivalent ions along the polymer chains are responsible for the conformational collapse;[3,16–27] whereas, the reexpansion of the chains at very high multivalent salt concentrations is

[a)]Author to whom correspondence should be addressed. Electronic mail: chingih@ntu.edu.tw.

 © 2012 American Institute of Physics

Downloaded 23 Apr 2012 to 140.112.148.95. Redistribution subject to AIP license or copyright; see http://jcp.aip.org/about/rights_and_permissions

mainly attributed to the screening effects of the electrostatic interactions between monomers.[3,16,20–22] Moreover, some of the theoretical studies have addressed the degree of reexpansion, relating it to the overcharge of the polyelectrolytes caused by the condensed ions.[20,24,27] However, Solis proposed that when considering the association of counterions and co-ions to the polyelectrolyte chains at high salt concentrations, it is possible for these reexpanded or redissolved chains to have either sign of the total effective charge.[23] Later, Hsiao predicted that the association of co-ions becomes more significant in the presence of larger salt counterions using the coarse-grained molecular dynamics simulation method.[25,26] These adsorbed counterions and co-ions tend to form a multilayer organization around a polymer chain, as proposed by Solis.[23] The resultant chains are more elongated and do not show a collapsed transition at the intermediate salt concentrations when the size of the multivalent salt ions is significantly larger than that of the monomers. The most compact or collapsed chain conformation was observed when the salt ions have a comparable size with the monomers. Though current theoretical studies have captured most of the phenomena associated with the conformational variation in polyelectrolytes, the effects that involve the local arrangement of the condensed salt counterions, co-ions, and the solvent molecules around the polyelectrolyte chain have not yet been addressed.

Despite computer simulations that have been used to study the conformational behavior at an atomistic scale, most of them are based on the so-called coarse-grained model.[24–26,28–36] We thus used all-atom molecular dynamics (MD) simulations to examine the condensation behavior of salts, co-ions, local structure, and dynamics of water in the vicinity of a single polyelectrolyte chain. In particular, we considered a single molecule of syndiotactic poly(methacrylic acid) (PMAA) chain in an aqueous solution at various values of salt concentration. The *p*H dependency of PMAA molecular conformation and corresponding properties make it useful for biomedical and industrial applications.[6,8,9,37–39] Previously, we ignored the existence of any type of counterions and addressed the associated effects of the local arrangement and the dynamic behavior of water molecules surrounding the high hydrophilic COO^- and low hydrophilic COOH functional groups along the polymer chain.[40] We showed that because of the strong attractions between water and charged monomers, the water molecules form highly bonded structures surrounding the chain through the formation of hydrogen bonds. Furthermore, water molecules often act as a bridging agent between two neighboring COO^- groups. These bridged water molecules were observed to stabilize the rod-like chain conformation, which is a character of the highly charged chain, as they significantly limit torsional and bending degrees of the backbone monomers. In addition, they display different dynamic properties from the bulk water. Both the resultant oxygen and hydrogen spectra are greatly shifted because of the strong H-bonded interactions.

In this study, to examine the conformational behavior of a polyelectrolyte chain as well as the dynamical properties of water in the presence of salts, all the COOH groups along the PMAA chain were replaced by COONa, which is 100% dissociated into COO^- and Na^+, as presented in Fig. 1. By doing so, we examined the condensation behavior of these monovalent Na^+ counterions within the chain and its influence on the chain conformational behavior and dynamics of water molecules. We then simulated the salt-dependent conformational behavior of the single sodium PMAA chain in aqueous solutions by adding various concentrations of multivalent $CaCl_2$. Finally, when examining the water distribution as well as the dynamic properties of water surrounding the polymer chain in the presence of the condensed counterions, we analyzed the radial distribution function (RDF) of water molecules with respect to COO^- functional groups, and the self-velocity autocorrelation function (VACF) and the vibration spectra of water molecules.

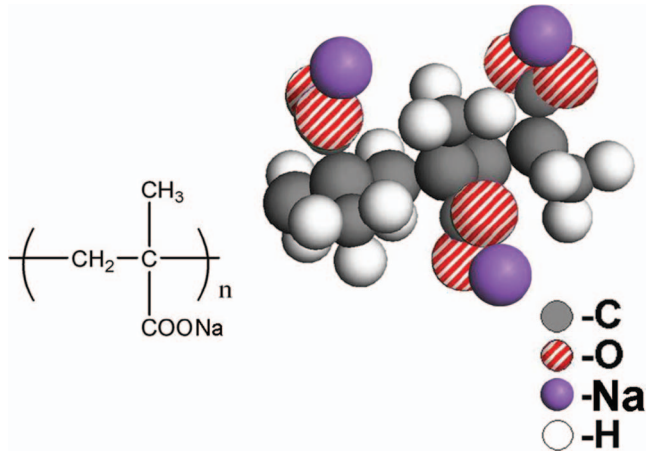

FIG. 1. Schematic representation of PMAA structure with all COOH replaced by COONa and 100% dissociated into COO^- and Na^+.

II. MODEL AND SIMULATION METHODS

We adopted the COMPASS force-field method of the Discover module in the Materials Studio (MS) molecular modeling software, which is an all-atom model, to calculate the atomic interaction parameters.[41,42] The total potential energy function U is given as follows:

$$U = U_{\text{internal}} + U_{\text{cross}} + U_{\text{non-bond}}, \tag{1}$$

where U_{internal} and U_{cross} represent the bonded interactions contributed from the internal-coupling and cross-coupling terms, respectively, and $U_{\text{non-bond}}$ represents the non-bonded interactions. These terms have the following forms:

$$\begin{aligned} U_{internal} = &\sum_b [{}^2K_b(b-b_0)^2 + {}^3K_b(b-b_0)^3 + {}^4K_b(b-b_0)^4] \\ &+ \sum_\theta [{}^2K_\theta(\theta-\theta_0)^2 + {}^3K_\theta(\theta-\theta_0)^3 \\ &+ {}^4K_\theta(\theta-\theta_0)^4] \\ &+ \sum_\phi [{}^1K_\phi(1-\cos\phi) + {}^2K_\phi(1-\cos 2\phi) \\ &+ {}^3K_\phi(1-\cos 3\phi)] + \sum_\chi K_\chi \chi^2, \end{aligned} \tag{2a}$$

Downloaded 23 Apr 2012 to 140.112.148.95. Redistribution subject to AIP license or copyright; see http://jcp.aip.org/about/rights_and_permissions

$$
\begin{aligned}
U_{cross} = & \sum_{b}\sum_{b'} K_{bb'}(b-b_0)(b'-b_0') \\
& + \sum_{\theta}\sum_{\theta'} K_{\theta\theta'}(\theta-\theta_0)(\theta'-\theta_0') \\
& + \sum_{b}\sum_{\theta} K_{b\theta}(b-b_0)(\theta-\theta_0) \\
& + \sum_{b}\sum_{\phi}(b-b_0)({}^1K_{b\phi}\cos\phi + {}^2K_{b\phi}\cos 2\phi \\
& + {}^3K_{b\phi}\cos 3\phi) \\
& + \sum_{\theta}\sum_{\phi}(\theta-\theta_0)({}^1K_{\theta\phi}\cos\phi + {}^2K_{\theta\phi}\cos 2\phi \\
& + {}^3K_{\theta\phi}\cos 3\phi) \\
& + \sum_{\phi}\sum_{\theta}\sum_{\theta'} K_{\phi\theta\theta'}(\theta-\theta_0)(\theta'-\theta_0')\cos\phi, \quad (2b)
\end{aligned}
$$

$$
U_{non-bond} = \sum_{i,j}\frac{q_i q_j}{r_{ij}} + \sum_{i,j}\epsilon_{ij}\left[2\left(\frac{r_{ij}^{\circ}}{r_{ij}}\right)^9 - 3\left(\frac{r_{ij}^{\circ}}{r_{ij}}\right)^6\right]. \quad (2c)
$$

In Eqs. (2a) and (2b), b, θ, ϕ, and χ represent the internal coordinates of the bond length, bending angle, torsion angle, and out-of-plane angle, respectively, with the subscript 0 denoting the corresponding equilibrium values when energy is at a minimum value. The terms of ${}^2K_b$, ${}^2K_\theta$, $K_{b\theta}$, and other terms are the related force constants. The cross-coupling terms in Eq. (2b), which include combinations of two or three internal coordinates, are important for determining structural variations and vibration frequencies associated with the conformational changes. In Eq. (2c), the non-bonded interaction term ($U_{\text{non-bond}}$) is composed of Lennard-Jones 9-6 van der Waals interactions and electrostatic Coulomb potential energy, where q_i and q_j are the partial charges of the ith and jth atoms, ε_{ij} corresponds to the energy parameter between i and j, and r_{ij} and r_{ij}° represent the distance and equilibrium distance between the ith and jth atoms, respectively.

The system consists of a single chain of 100% charged syndiotactic PMAA with a degree of polymerization of N equal to 48. When maintaining the electrically neutral state, 48 Na^+ counterions were added instead of H^+, as presented in Fig. 1. The PMAA chain was first put in a vacuum box with a side length of 50 Å and a periodic boundary condition and then the box was gradually filled with approximately 2800 water molecules. After that, various numbers of $CaCl_2$ (12, 18, 24, 30, 36, 48, 72, 120, 180, and 240) were added to the system, which the numbers correspond to the molar concentrations of salt (Cs) equal to 0.16, 0.24, 0.32, 0.40, 0.48, 0.64, 0.96, 1.60, 2.4, and 3.2 M, respectively. The molecular dynamics simulations were performed by integrating the positions and velocities of all atoms according to the velocity-Verlet algorithm.[43,44] The integration time step was chosen as 1 fs, and the initial temperature was set at 300 K. We adopted the accurate Ewald summation, in which the long-range interactions are treated to include interactions of the periodic images. Prior to simulation, the steepest descent minimization method was used to relax and equilibrate the initial structure. In more detail, the PMAA chain was fixed and the water solvent was relaxed to populate the relevant hydration sites on the PMAA for 30 ps in a canonical *NVT* ensemble. This minimized structure was then performed by a series of annealing processes. The annealing temperature was first raised from 300 to 600 K at a rate of 3 K/ps and kept at 600 K for 100 ps. It was then quenched to 300 K at the same rate and kept at 300 K for 20 ps. This annealing cycle was repeated four to six times to assure that the system had been equilibrated. Finally, it was followed by a long relaxation period of 500 ps at 300 K. After performing these processes so that the system's energy reached the equilibrium value, we analyzed the radius of gyration (R_g) of the PMAA chain and the RDF every 100 fs, as well as the self-VACF of water molecules every 5 fs, which were averaged out for the data collection intervals of 50 ps.

To examine the dynamic behavior of water molecules, we calculated the VACF, as defined by

$$
G(\tau) = \frac{\langle v_i(t_0)\cdot v_i(t_0+\tau)\rangle}{\langle v_i(t_0)\cdot v_i(t_0)\rangle}, \quad (3)
$$

where, t_0 and τ correspond to reference and delay times, respectively, and $v_i(t)$ is the atomic velocity at time t. The average was carried over atoms of the same type and the reference time for the 50 ps period of data collection. Once the VACF profiles of the O and H atoms of water were obtained, the vibration spectra of O and H were analyzed by applying the Fourier transformation to the VACF profiles.[45]

III. RESULTS AND DISCUSSION

In this study, our results are divided into the following parts. We first examined how the PMAA chain conformation varies with the concentration of $CaCl_2$(C_S). We then investigated the local condensation behavior of Na^+ and Ca^{2+} associated with the co-ion Cl^- and the influences on the chain conformation. Finally, we discussed how the distribution and dynamic properties of water molecules are affected in the presence of the condensed salt ions.

Prior to presenting the results, we described the criteria to determine the ion condensation surrounding the chain as well as the formation of ionic bonds between the salt ions and water molecules and hydrogen bonds between the COO^- and water in our analysis. The metal ions are defined as "condensed" when the distance between the O atoms of COO^- groups and the ions is smaller than 2.5 Å. The value of 2.5 Å is close to the summation of the van der Waals radius of one O^{2-} (1.40 Å) and one ion (1.02 Å for Na^+ and 1.00 Å for Ca^{2+}, respectively). The later analysis of the RDF profiles of Na^+ and Ca^{2+} with respect to the O atoms in the COO^- groups will show a strong peak at 2.0 Å, supporting the determination of ionic bonding between the ion and COO^- used here. Similarly, the formation of ionic bonds between the salt ions and the O atoms in the water is determined by the aforementioned criteria. When forming the hydrogen bonds between the COO^- and water, the distance between the O atoms in the COO^- and the H atoms in the water is less than the normal hydrogen bonding length of 1.8 Å.[40] This value of 1.8 Å is close to the first peak position (1.5 Å) of the RDF profile of

Downloaded 23 Apr 2012 to 140.112.148.95. Redistribution subject to AIP license or copyright; see http://jcp.aip.org/about/rights_and_permissions

the hydrogen in the water with respect to the O atoms in the COO^- groups.

A. Effects of $CaCl_2$ concentration on the polymer conformation

The molecular conformational behavior of polymer chains is analyzed by calculating the radius of gyration, which is defined as

$$R_g = \langle R_g^2 \rangle^{1/2} = \left\langle \frac{1}{N} \sum_{i=1}^{N} |\vec{r}_i - \vec{r}_{cm}|^2 \right\rangle^{1/2}, \quad (4)$$

where $\vec{r}_i$ and $\vec{r}_{cm}$ represent the position vector of the ith atom and the center of mass of the PMAA, respectively. For the same polymer, a larger value of R_g corresponds to a more stretched polymer chain. Figure 2 displays the variation of R_g with C_S, where the maximum and minimum values of R_g are designated with error bars. Similar to other theoretical studies,[24–27] we obtained the same trend that with the increase of $CaCl_2$ concentration, R_g decreased to a minimum value at $Cs = 0.48$ M, and after increasing, leveled off at a certain value. To clearly investigate the significant effects contributed from the Na^+ and Ca^{2+} ions, we repeated the same simulation, but without any type of counterions, and obtained the corresponding value of R_g approximately 14.8 Å. In this case, the PMAA chain exhibited a more rod-like conformation because of the repulsive electrostatic interactions between the charged COO^- groups. We previously reported that the water molecules often act as a bridging agent between two neighboring COO^- groups and stabilize the rod-like conformation.[40] When Na^+ ions were added to maintain electrically neutral ($Cs = 0$, no $CaCl_2$), the resultant value of the R_g was approximately 12.4 Å, indicating a more coil-like conformation than for a strongly charged chain in the dilution limit. In Table I, we list the respective numbers of each type of condensed Na^+ and Ca^{2+} ions obtained at various $CaCl_2$ concentrations, $Na^+_{(S)}$, $Na^+_{(C)}$, $Ca^{2+}_{(S)}$, and $Ca^{2+}_{(C)}$, which are stretched-type (with subscript s) and coiled-type (with subscript c), respectively. The numbers of condensed Na^+ and Ca^{2+} ions are equal to $Na^+_{(S)} + Na^+_{(C)}$ and $Ca^{2+}_{(S)} + Ca^{2+}_{(C)}$, respectively. The listed numbers for each type of condensed ions were obtained by averaging the simulation results during a data collection interval of 50 ps. The stretched-type and coiled-type of the condensed ions will be explained in more detail later. As presented in Table I, there were around 28 out of the total present 48 Na^+ ions condensed into the chain when $C_S = 0$. As expected, owing to the significant condensation of monovalent counterions Na^+, the repulsions between the COO^- groups were screened significantly and R_g became smaller. By adding $CaCl_2$, we found

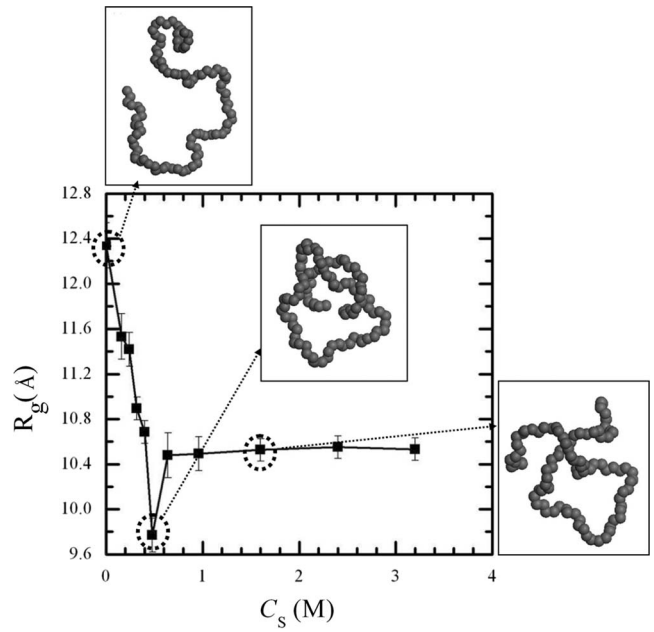

FIG. 2. Plot of the radius of gyration (R_g) of PMAA versus concentration of $CaCl_2$ (C_S). Several snapshots of the equilibrium chain conformation of PMAA are also displayed by only showing the backbone carbon atoms.

TABLE I. Variation in the number of each type of condensed ions, which are stable surrounding the COO^- groups during a data collection interval of 50 ps, with the concentration of $CaCl_2(C_S)$. The corresponding total added numbers of Ca^{2+} with respect to each concentration in the system are presented in the brackets. $Na^+_{(S)}$, $Na^+_{(C)}$, $Ca^{2+}_{(S)}$, and $Ca^{2+}_{(C)}$ are stretched-type (with subscript s) and coiled-type (with subscript c) of the condensed Na^+ and Ca^{2+} ions, respectively.

C_S (M) (Number of added Ca^{2+})	$Na^+_{(S)}$	$Na^+_{(C)}$	$Na^+_{(S)} + Na^+_{(C)}$	$Ca^{2+}_{(S)}$	$Ca^{2+}_{(C)}$	$Ca^{2+}_{(S)} + Ca^{2+}_{(C)}$	Net charge within the chain
0 (0)	17.86	10.03	27.89	0	0	0	− 20.11
0.16 (12)	12.92	8.88	21.80	4.02	1.05	5.07	− 16.06
0.24 (18)	13.13	7.11	20.24	3.06	4.08	7.14	− 13.48
0.32 (24)	10.02	9.16	19.18	5.89	3.01	8.90	− 11.02
0.40 (30)	9.98	8.04	18.02	5.11	5.23	10.34	− 9.30
0.48 (36)	7.86	9.32	17.18	1.98	9.22	11.20	− 8.42
0.64 (48)	6.07	8.01	14.08	9.03	4.95	13.98	− 5.96
0.96 (72)	6.98	5.27	12.25	8.96	8.01	16.97	− 1.81
1.6 (120)	6.10	4.05	10.15	9.96	11.97	21.93	+6.29
2.4 (180)	5.17	5.08	10.25	12.07	9.97	22.04	+6.33
3.2 (240)	3.97	3.94	7.91	12.11	12.03	24.14	+8.19

Downloaded 23 Apr 2012 to 140.112.148.95. Redistribution subject to AIP license or copyright; see http://jcp.aip.org/about/rights_and_permissions

that more Ca^{2+} ions were condensed surrounding the PMAA instead of Na^+ when the salt concentration C_S kept increasing (Table I). This is reasonable because of stronger attractive interaction between Ca^{2+} and COO^- than that between Na^+ and COO^-. Thus, the bridging effects associated with the condensation of multivalent salt ions make the chain more coiled and collapsed. However, R_g does not show a continuously decreasing behavior with C_S through the entire range of the salt concentration examined here, in which more Ca^{2+} ions are condensed. One may think the reexpansion of polyelectrolyte chain when $C_S > 0.48$ M is attributed to the screening effect and the overcharging effect because of the excess condensation of ions. To examine this hypothesis, we calculated the net charge within the polymer chain by accounting for all the charged COO^- groups and the condensed salt counterions of Na^+ and Ca^{2+} into the COO^-, as listed in Table I. Clearly, net charge became positive at $C_S = 1.6$ M, which is significantly greater than the occurrence of chain expansion at 0.48 M. We found that the local organization of the condensed ions and water molecules surrounding the chain play important roles on the conformational behavior of polyelectrolyte chain. This issue, however, has not been addressed in the literature. We will show that when the salt concentration becomes significantly high ($C_S \geqq 1.6$ M), the counterions of Ca^{2+} and Na^+ and co-ions of Cl^- tend to form a shell-like multilayer organization outside the PMAA chain. This multilayer formation strongly limits the expansion degree of the polyelectrolyte chain conformation.

B. Condensation behavior of Na^+ and Ca^{2+} associated with Cl^- and the effects on the chain conformation

Generally, Na^+ can be adsorbed into the O atoms of either COO^- groups or water molecules. Depending on the relative size of the sodium and oxygen ions, we observed four O atoms to be attracted around one Na^+. This is similar to the frequently observed Na_2O crystal structure, in which a sodium ion has a coordination number of 4.[46] It is likely for a condensed Na^+ ion to attract more than one COO^- group and act as a bridging agent within the polymer chain. Figure 3 shows several characteristic arrangements of the condensed Na^+ ions around the PMAA chain with COO^- groups, in which there is no addition of $CaCl_2$ ($C_S = 0$), for example. In particular, parts (a) and (b) of Fig. 3 demonstrate a frequently observed condensation behavior of Na^+ into two COO^- groups, but have different influence on the resultant local chain conformation. In Fig. 3(a), Na^+ is strongly bonded to the two O atoms of 1 and 2, which belong to two adjacent COO^- groups. This condensed Na^+ is able to limit the torsional and bending degrees of the backbone monomers and to contribute to the formation of the locally stretched conformation. Though similar bridging behavior via the condensed Na^+ has been observed in Fig. 3(b), bonding to two non-neighboring COO^- groups causes the chain to fold locally. Figures 3(c) and 3(d) present the local arrangement of Na^+ bonded to three adjacent and non-adjacent COO^- groups, respectively. We clearly observed a local rod-like conformation in Fig. 3(c), where the adsorption of Na^+ attracts the O atoms

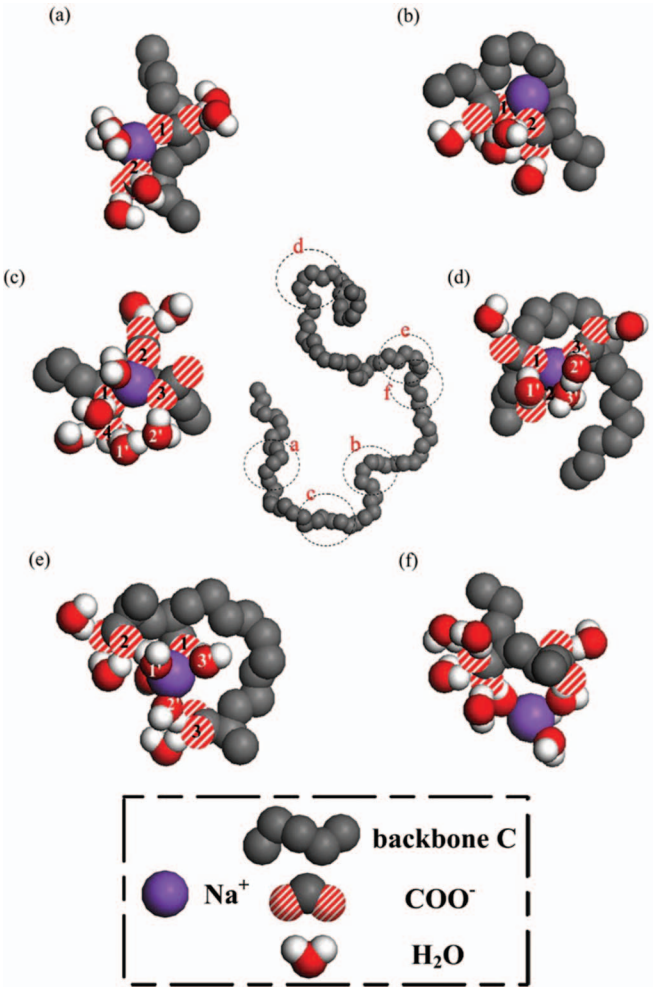

FIG. 3. Snapshots of characteristic arrangements of condensed Na^+ ions and water molecules around the COO^- functional groups, taken from a PMAA macromolecular chain when $C_S = 0$ (without the addition of $CaCl_2$). In the center part, the equilibrium chain conformation of PMAA is displayed by only showing the backbone carbon atoms.

designated as 1, 2, and 3, in the three sequential COO^- groups to form a stable triangle. Moreover, there are water molecules, designated as 1′ and 2′, which act as a bridging agent between the pairs of 3–4 O atoms via hydrogen bonding, and stabilize the local arrangement behavior of the adsorbed Na^+ with respect to the COO^- groups. When Na^+ is condensed around the three O atoms in the non-neighboring COO^- groups, as shown in Fig. 3(d), a locally coiled conformation is observed. This conformational behavior is enhanced by the local bridging arrangement of water molecules, for example, 1′ between the O atoms 1 and 2 in the COO^- groups, 2′ and 3′ between Na^+ and the O atom, 3 in the COO^- groups. In addition to the condensation of Na^+ around two and three COO^- groups, it has been observed to be bonded to one COO^- and three water molecules, as shown in Fig. 3(e), and to four water molecules without directly bonded to COO^-, as shown in Fig. 3(f). In Fig. 3(e), Na^+ is directly bonded to the O atom 1, and the three O atoms 1′, 2′, and 3′, which belong to the COO^- groups and water, respectively. We found these attracted water molecules bridge between Na^+ and the O atom 2 in its neighboring COO^- monomers and between Na^+ and the

Downloaded 23 Apr 2012 to 140.112.148.95. Redistribution subject to AIP license or copyright; see http://jcp.aip.org/about/rights_and_permissions

O atom 3 in the farther COO^- monomers. Accordingly, the resultant local chain conformation becomes coil-like. Note that the water molecules are also possible to bridge only between Na^+ and adjacent COO^- monomers, and cause a locally stretched conformation. For example in Fig. 3(f), though Na^+ is not condensed directly into any COO^- groups, it is closely around the chain through the water molecules bridging between Na^+ and COO^- groups. These water molecules associated with Na^+ form a huge cluster between the neighboring COO^- groups, which develops a locally stretched conformation.

From this discussion, it is reasonable to conclude that along with the water molecules, the condensed Na^+ ions often act as a bridging agent between the COO^- groups in the polymer chain. They are classified into two characteristic types. One coiled-type of condensed sodium ions, designated as $Na^+_{(C)}$, tends to bridge between "non-adjacent" COO^- functional groups and causes the chain locally coiled or bended. The other stretched-type $Na^+_{(S)}$ provides a bridging effect between "adjacent" COO^- groups and causes a locally stretched chain conformation. As listed in Table I, the numbers of each type of $Na^+_{(C)}$ and $Na^+_{(S)}$ decrease with an increase in the $CaCl_2$ concentration of C_S. What follows is the condensation behavior of multivalent Ca^{2+} salt ions, which plays a more dominant role in the chain conformation.

When forming the ionic bonds between the calcium and oxygen ions, we observed six O atoms to be attracted around one Ca^{2+}.[46] Thus, the number of the O atoms in the COO^- groups that Ca^{2+} is bonded to in our simulations varies from 0 to 6. We consider $C_S = 0.96$ M as an example to display the typical arrangements of the condensed Ca^{2+} salt ions around the PMAA chain with COO^- groups in Fig. 4. Typically, when Ca^{2+} is condensed to one and two O atoms in the COO^- groups, as shown in parts (a) and (b) of Fig. 4, respectively, a locally stretched chain conformation is often observed. When Ca^{2+} attracts four, five, and six O atoms of the COO^- groups, as shown in parts (c)–(e) of Fig. 4, respectively, its condensation often pulls far COO^- groups together and causes a locally coiled conformation. When Ca^{2+} is condensed to three O atoms in the COO^- groups, condensation with adjacent and non-adjacent COO^- groups are possible, and the resultant chain conformation is either locally stretched or coil-like, as shown in parts (f and g) of Fig. 4, respectively. In general, as Ca^{2+} provides a stronger attraction with COO^- or water, these directly bonded water molecules are more difficult to get bridged to other groups (such as COO^-). The neighboring COO^- groups are more difficult to adsorb water molecules. Accordingly, a bridging phenomenon through the water molecules is seldom observed, as has been observed in the condensation of Na^+. Instead, these condensed multivalent salt ions Ca^{2+} provide a strong bridging effect within the polymer chain. Thus, in our simulations we did not observe that Ca^{2+} was attracted within the chain without directly bonding to COO^- but only through the bridging of water molecules.

The salt counterions of Ca^{2+} and Na^+ attract COO^- groups and water molecules as well as the Cl^- co-ions. When the $CaCl_2$ concentration is lower than 0.48 M, in which the chain conformation is the most coil-like (collapsed), we did not observe any Cl^- co-ions within or surrounding the PMAA chain. As C_S increases from 0.48 M such that the chain starts to expand from the most collapsed state, more Cl^- co-ions are observed surrounding the PMAA chain. For example, in Fig. 5, we display the resultant PMAA backbone chain as well as the Cl^- ions within a 5 Å distance surrounding the backbone chain at $C_S = 3.2$ M. As expected, these Cl^- ions tend to be close to the PMAA chain from Coulomb electrostatic force with Ca^{2+} or Na^+ ions, which are directly condensed into the COO^- groups. The associated Ca^{2+} and Na^+ ions are condensed to either one or two O atoms in the COO^- groups because of the presence of Cl^-. For example, in part (a) of Fig. 5, we illustrate the attachment of Cl^- into the Ca^{2+} and Na^+, which are bonded to the O atom (designated as 1) and the two O atoms (designated as 2 and 3) in the COO^- groups, respectively. In part (b) of Fig. 5, the Cl^- co-ions are associated with the condensed Ca^{2+} and Na^+ into two and one O atoms in the COO^- groups, respectively. Obviously, these counterions, co-ions, and the surrounding water molecules form huge clusters outside the chain to stabilize the locally stretched conformation. By analyzing in detail the trend of the number of each type of the condensed salt ions, which results in a locally coiled-like and stretched-like conformation,

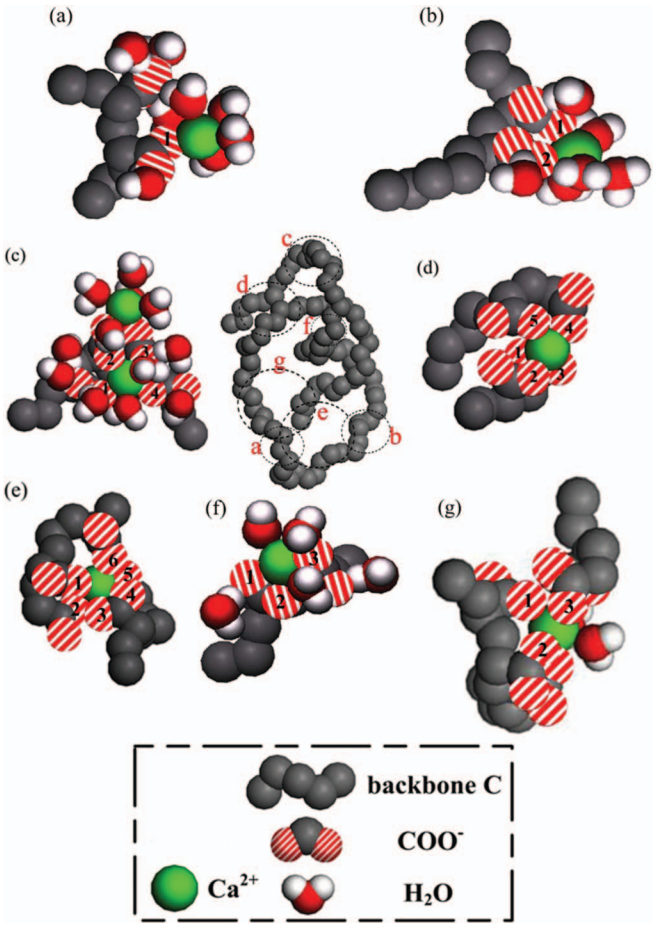

FIG. 4. Snapshots of characteristic arrangements of condensed Ca^{2+} ions and water molecules around the COO^- functional groups, taken from a PMAA macromolecular chain when $C_S = 0.96$ M. In the center part, the equilibrium chain conformation of PMAA is displayed by only showing the backbone carbon atoms.

Downloaded 23 Apr 2012 to 140.112.148.95. Redistribution subject to AIP license or copyright; see http://jcp.aip.org/about/rights_and_permissions

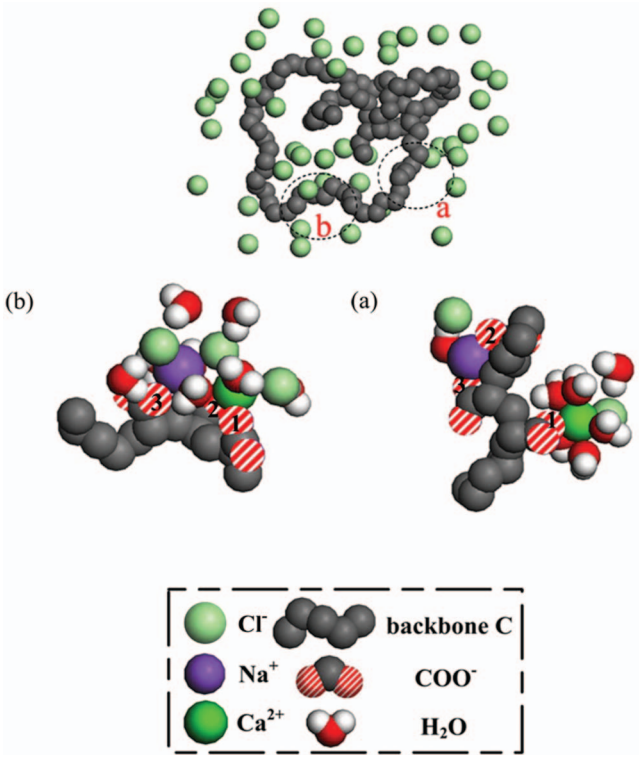

FIG. 5. Snapshots of characteristic arrangements of condensed salt ions and Cl^- co-ions around the COO^- functional groups, taken from a PMAA macromolecular chain when $C_S = 3.2$ M. In the upper part, the equilibrium chain conformation of PMAA is displayed by showing the backbone carbon atoms and the nearby Cl^- co-ions.

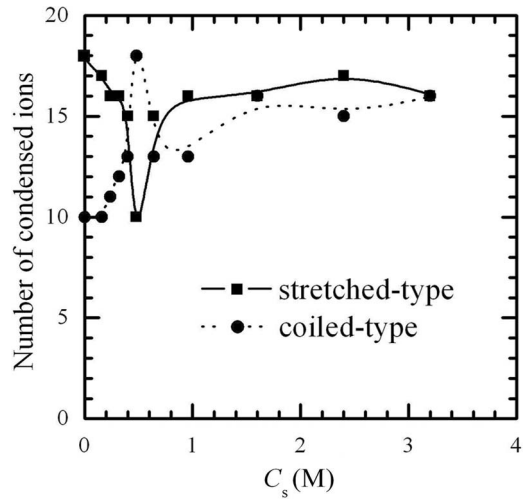

FIG. 6. Plot of the numbers of stretched-type ($Na^+_{(S)} + Ca^{2+}_{(S)}$) and coiled-type ($Na^+_{(C)} + Ca^{2+}_{(C)}$) condensed ions as a function of the concentration of $CaCl_2$ (C_S).

respectively, as a function of C_S, we found a significant increase of the stretched-type condensed salt ions in the expanded conformation regime. This observation is mainly attributed to the association of the Cl^- co-ions.

As listed in Table I, when the $CaCl_2$ concentration of C_S increases, the trends of the coiled-type $Ca^{2+}_{(C)}$ and the stretched-type $Ca^{2+}_{(S)}$ show a roughly local maximum and minimum, respectively. At $C_S = 0.48$ M, the PMAA chain displays the most coiled conformation. Both numbers of the coiled-type $Na^+_{(C)}$ and the stretched-type $Na^+_{(S)}$ show a decreasing trend with the salt concentration C_S. When plotting the number of each stretched-type ($Na^+_{(S)} + Ca^{2+}_{(S)}$) and coiled-type ($Na^+_{(C)} + Ca^{2+}_{(C)}$) ions as a function of C_S, as shown in Fig. 6, we observed an accordance with the resultant R_g behavior in Fig. 2. When R_g shows a decreasing trend and reaches a local minimum with the increase of C_S until 0.48 M, the number of coiled-type of condensed ions increases to a maximum value; whereas, the stretched-type shows an opposite trend. It should be noted that our results do not show that the most collapsed conformation occurs when the net charge becomes zero. As shown in Table I, this occurs before the chain becomes electrically neutral (the net charge within the chain is -8.4 at $C_S = 0.48$ M). When C_S increases further and ranges between 0.48 M and 0.96 M, the net charge becomes less negative and the smaller repulsive electrostatic interactions support the formation of a more collapsed or coiled conformation. While, a significant increase in the amount of stretched-type rather than the coiled-type condensed ions forms an expansion effect on the chain. Our results have shown that the reexpansion of the chain conformation at high salt concentrations is attributed to the overcharging effect and to the substantial amounts of the condensed ions that result in a locally stretched conformation. Moreover, when the salt concentration continues to increase further into the regime of $C_S > 0.96$ M, the number of the stretched-type condensed ions increases to a value slightly larger than the coiled-type ions. This significant increase in the amount of the condensed Ca^{2+} and Na^+ ions often occurs outside the PMAA chain associated with a large amount of the Cl^- co-ions to get nearby, as shown in Fig. 5.

To analyze quantitatively how the Cl^- co-ions and the salt counterions of Ca^{2+} and Na^+ distribute around the COO^-, we calculated the RDF of these ions with respect to the O atom in the COO^- groups. The RDF ($g_{A\text{-}B}(r)$) indicates the local probability density of finding B atoms at a distance r from A atoms averaged over the equilibrium density, as follows:

$$g_{A-B}(r) = \frac{n_B/4\pi r^2 dr}{N_B/V}, \tag{5}$$

where n_B is the number of B atoms at a distance r in a shell of thickness dr from atom A, N_B is the total number of B atoms in the system, and V is the total volume of the system. Figures 7(a) and 7(b) show the corresponding RDF profiles of the sum of Ca^{2+} and Na^+, and Cl^-, respectively, as a function of C_S. Noticeably, a strong peak associated with a second peak for the RDF profile of the salt counterions appear at 2.0 and 4.1 Å, suggesting that a significant amount of the salt ions condense and form a shell-like layer around the COO^- groups for the entire regime of the salt concentrations examined here. When $C_S \geqq 1.6$ M, we observed two sharp peaks for the Cl^- RDF profile at 3.4 and 4.7 Å. These results have suggested that at this high salt concentration regime, the counterions of Ca^{2+} and Na^+ and co-ions of Cl^- tend to form a multilayer organization outside the surrounding of the PMAA chain. The expansion degree of the polyelectrolyte chain conformation is greatly limited, as observed in the R_g behavior (Fig. 2).

Downloaded 23 Apr 2012 to 140.112.148.95. Redistribution subject to AIP license or copyright; see http://jcp.aip.org/about/rights_and_permissions

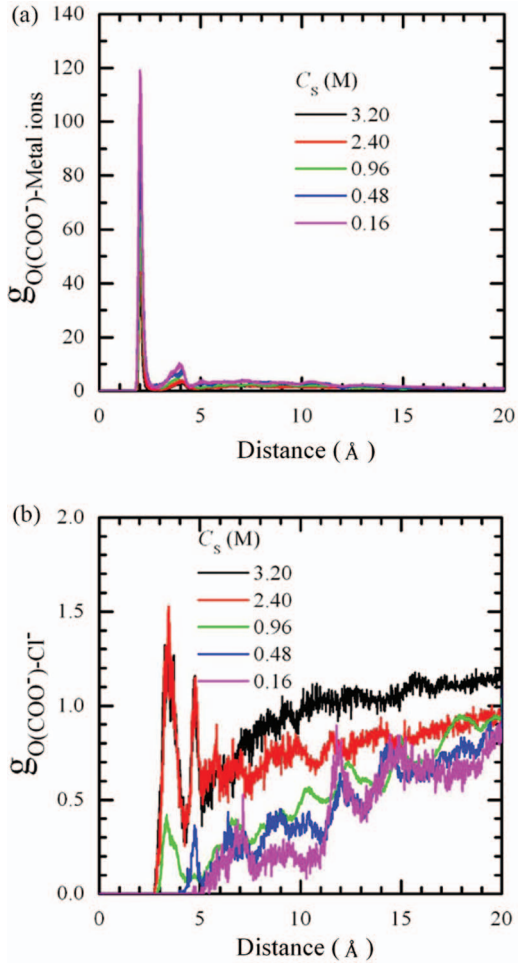

FIG. 7. The radial distribution functions of (a) the sum of Ca^{2+} and Na^+ and (b) Cl^- with respect to the O atoms in the COO^- functional groups as a function of $CaCl_2$ concentration (C_S).

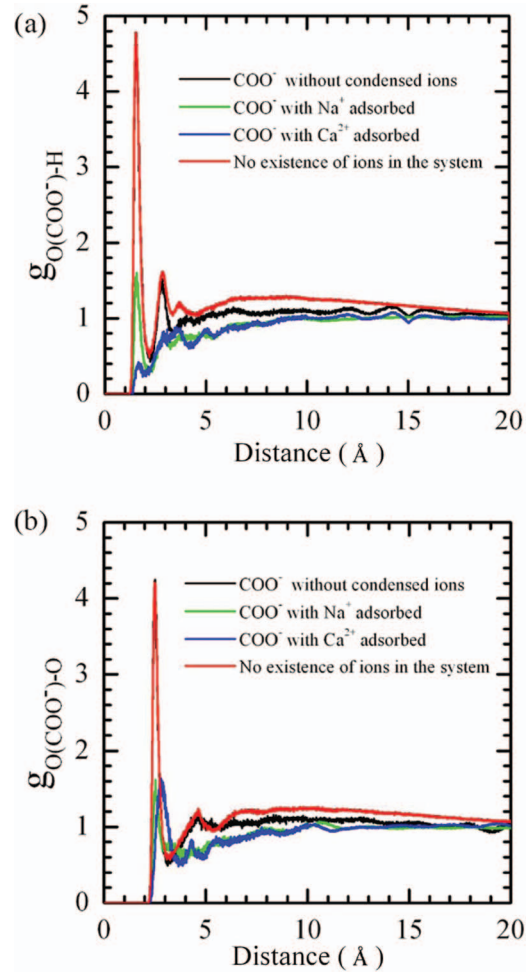

FIG. 8. The radial distribution functions of (a) hydrogen and (b) oxygen atoms of water with respect to the O atoms in the various types of COO^- functional groups when $C_S = 0.64$ M.

C. Distribution of water molecules in the presence of condensed salt ions

In aqueous solutions, the hydration behavior of molecules is complex but worthwhile for further exploration. As discussed via the snapshots of the local PMAA chain, the condensation behavior of salt ions, local arrangement of water molecules, and the PMAA chain conformation are strongly associated with each other. Consequently, the local distribution and the resultant dynamic behavior of water molecules surrounding the PMAA chain differ with and without the condensed salt ions.

Figures 8(a) and 8(b) show the corresponding RDF profiles of the hydrogen and oxygen of water with respect to the O atoms in the COO^- groups, respectively, when $C_S = 0.64$ M. In the system, the COO^- groups are classified into three types: without any condensation of ions, with a condensation of Na^+ ion, and with a condensation of Ca^{2+}. Once water distribution surrounding the COO^- functional groups was analyzed without any condensed counterions, we observed two prominent peaks at 1.5 Å and 2.8 Å for the hydrogen RDF profile and one peak at 2.5 Å for the oxygen RDF profile, suggesting that a shell-like layer of water molecules forms around the COO^- groups. These RDF profiles are similar to those obtained from the same charged PMAA chain in an aqueous solution but without any type of counterions (i.e., the solution is not electrically neutral), which has been reported previously[40] and displayed here for comparison. When considering a Na^+ ion condensed into the COO^- group, each resultant RDF profile of H and O atoms was observed to exhibit only a clear peak with the same position as in the case without any condensed ions surrounding the COO^- groups but with a significantly lower height. That is to say, though the condensation of Na^+ ion causes a decrease in the distribution of water molecules surrounding the COO^- groups, a substantial amount of water molecules are still attracted surrounding the COO^- groups through the formation of hydrogen bonds. When the condensed salt ions are multivalent (Ca^{2+}), because Ca^{2+} provides a stronger attraction with COO^- or water, most of the water molecules have been observed to be bonded directly to Ca^{2+} through the O atoms. Accordingly, the resultant hydrogen RDF profile does not show any obvious peaks. We only observed a peak for the oxygen RDF profile at 2.8 Å, which is slightly larger than the typical value of 2.5 Å when forming the hydrogen bonds between the COO^- and water.

The water molecules surrounding the charged PMAA chain in the presence of salt ions are adsorbed to the COO^-

Downloaded 23 Apr 2012 to 140.112.148.95. Redistribution subject to AIP license or copyright; see http://jcp.aip.org/about/rights_and_permissions

groups via the hydrogen bonds with the H atoms and to the counterions (Na^+ and Ca^{2+}) through the ionic bonds with the O atoms. Thus, the water molecules are classified into the following states: bulk water (designated as W0); water with one H atom bonded with the COO^- (W1); water with two H atoms bonded with the COO^- groups (W2); water with the O atom bonded with Na^+ (further divided into W0-Na^+, W1-Na^+, and W2-Na^+); and water with the O atom bonded with Ca^{2+} (further divided into W0-Ca^{2+}, W1-Ca^{2+}, and W2-Ca^{2+}). For example, W1-Na^+ represents the water molecule with one H atom bonded with the COO^- group and with the O atom bonded with Na^+. Other terms were defined similarly. The H and O atoms of water are designated following the type of water molecules. For example, in the type of W1-Na^+ water molecules, the O atom is designated as O1-Na^+, and the two H atoms are designated as H1y-Na^+ and H1n-Na^+, which correspond to the hydrogen-bonded and non-hydrogen-bonded types, respectively.

We list the fractions of each type of water molecules in Table II, which are stable during a data collection interval of 50 ps. It is interesting to find that in the presence of salt ions, water molecules tend to adsorb surrounding only one COO^- (W1 type), one Na^+ (W0-Na^+), or one Ca^{2+} (W0-Ca^{2+}). This is unlike previously reported cases without the existence of salt ions in the solutions, in which a significant amount of water molecules are able to bridge between the two COO^- functional groups (W2).[40] When only the monovalent Na^+ ions are present in the solutions (i.e., $C_S = 0$), there are roughly the same amount of W1 and W0-Na^+ water molecules (∼0.03). With an increase in the concentration of multivalent Ca^{2+} ions (C_S), the amount of W0-Na^+ molecules remains the same (∼0.04); and more water molecules are adsorbed into Ca^{2+} (W0-Ca^{2+}), as expected. For the entire regime of C_S examined here, there are few W2, W1-Na^+, and W1-Ca^{2+}. That is to say, few water molecules are bonded simultaneously with two COO^- functional groups or with one condensed salt ion and one COO^-.

We briefly summarized how the distribution of water molecules within the polymer chain is affected in the presence of the condensed salt ions. Two types of water molecules have been observed in the solutions: water with one H atom bonded with the COO^- and water with the O atom bonded with the condensed salt ion. Few water molecules are bonded simultaneously with two COO^- functional groups or with one condensed salt ion and one COO^-. When only the monovalent Na^+ ions are present in the solutions, water molecules are mainly adsorbed surrounding the condensed Na^+ ions or surrounding the COO^- groups. These adsorbed water molecules form hydrogen bonds to each other and enhance the local bridging behavior associated with the condensation of monovalent Na^+ ions on the resultant chain conformation. When more multivalent Ca^{2+} salt ions are added, because Ca^{2+} provides a stronger attraction with COO^- or water, more water molecules are bonded directly to the condensed Ca^{2+} ions with a small amount of water adsorbed into the condensed Na^+ ions. We observe no bridging phenomenon through the water molecules, as has been observed in the condensation of Na^+. Instead, only the condensed Ca^{2+} ions provide a strong bridging effect within the polymer chain.

D. Dynamics of water molecules in the presence of condensed salt ions

Figure 9 presents the time dependency of the VACF using Eq. (3) of the previously defined oxygen atom types, O0, O1, O2, O0-Na^+, O1-Na^+, O0-Ca^{2+}, and O1-Ca^{2+}. The negative region of these oxygen VACF profiles implies that these molecules have a greater probability of rebounding within this time. By integrating the VACF profiles for each type of oxygen atom in the water molecules, we compared the diffusion for each type of water molecules qualitatively. We previously showed a decreasing trend for the integrated values of O0, O1, and O2 (8.0×10^{-3}, 2.4×10^{-3}, and 1.5×10^{-3} ps, respectively), suggesting that the diffusion of water molecules slows

TABLE II. Fractions of each type of water molecules, which are stable during a data collection interval of 50 ps, at various $CaCl_2$ concentrations, C_S. The corresponding total added number of Ca^{2+} with respect to each concentration in the system are presented in the brackets. W0, W1, W2, W0-Na^+, W1-Na^+, W2-Na^+, W0-Ca^{2+}, and W1-Ca^{2+} represent the bulk water, water molecules adsorbed to COO^- with one or two H atoms, and the water molecules bonded with Na^+ or Ca^{2+} ions.

C_S (M) (Number of added Ca^{2+})	W1	W2	W0-Na^+	W1-Na^+	W2-Na^+	W0-Ca^{2+}	W1-Ca^{2+}	W0
0 (0)	0.032	0.006	0.033	0.007	0	0	0	0.922
0.16 (12)	0.036	0.004	0.045	0.001	0.0004	0.018	0.002	0.893
0.24 (18)	0.030	0.007	0.045	0.004	0.0007	0.029	0.002	0.883
0.32 (24)	0.024	0.0011	0.033	0.006	0	0.034	0.002	0.901
0.40 (30)	0.028	0.004	0.043	0.003	0	0.049	0.0011	0.871
0.48 (36)	0.025	0.005	0.043	0.004	0	0.059	0.003	0.861
0.64 (48)	0.025	0.004	0.043	0.002	0	0.074	0.005	0.847
0.96 (72)	0.022	0.004	0.045	0.003	0.0004	0.112	0.004	0.810
1.6 (120)	0.014	0.002	0.042	0.002	0.0004	0.202	0.008	0.731
2.4 (180)	0.008	0.002	0.045	0.003	0	0.207	0.005	0.730
3.2 (240)	0.009	0.0007	0.043	0.001	0.0004	0.267	0.007	0.672

Downloaded 23 Apr 2012 to 140.112.148.95. Redistribution subject to AIP license or copyright; see http://jcp.aip.org/about/rights_and_permissions

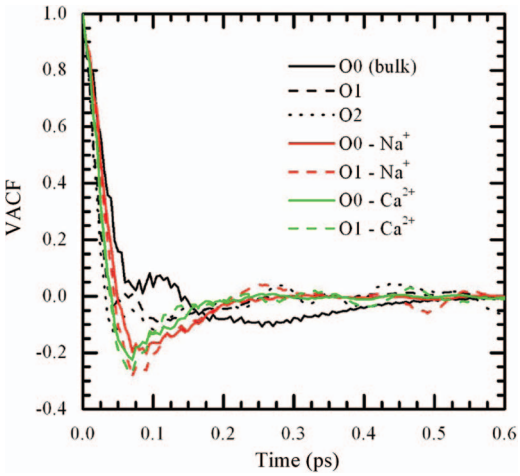

FIG. 9. The self-velocity autocorrelation functions (VACF) for oxygen atoms belonging to various types of water molecules in the system. O0, O1, O2, O0-Na^+, O1-Na^+, O0-Ca^{2+}, and O1-Ca^{2+} represent the oxygen atoms in bulk water, in water molecules adsorbed to COO^- with one or two H atoms, and in water molecules bonded with Na^+ or Ca^{2+} ions.

down with stronger attractions from the COO^- groups.[40] Similarly, with an increase in the attractions from the salt ions, a decreasing trend for the integrated values of O0, O0-Na^+, and O0-Ca^{2+} (8.0×10^{-3}, 2.6×10^{-3}, and 1.5×10^{-3} ps, respectively) was also observed. The W1-Ca^{2+} type of water molecules is expected to have the smallest diffusion coefficient by comparing the integrated values for O2, O1-Na^+, and O1-Ca^{2+} (1.5×10^{-3}, 8.8×10^{-4}, and 6.6×10^{-4} ps, respectively) when considering the effects associated with both COO^- and ions,.

Figures 10(a) and 10(b) present the vibration spectra of various types of oxygen and hydrogen for the water molecules with the O atom bonded with Na^+ but in different interaction states with the COO^-groups. We included the O0 and H0 spectra (i.e., bulk water) as a comparison. In Fig. 10(a), the O0 spectrum shows a major peak centered approximately at 58 cm^{-1} and a broad shoulder peak approximately at 200–300 cm^{-1}. Similar to the low frequency Raman spectra of liquid water reported by Walrafen *et al.*,[47] and other MD studies,[48–52] these results imply that the first peak is primarily associated with the non-H-bonded molecules; whereas the second broad peak is attributed to the H-bonded O-O intermolecular stretching vibration. When the water molecules are bonded with Na^+ (O0-Na^+, O1-Na^+), it is apparent that the bonding with Na^+ through the O atom provides a strong influence on the resultant oxygen spectra. In particular, the spectra shift towards higher wavenumber and the major spectrum peak becomes broader with a center approximately at 140 cm^{-1}. Moreover, when these Na^+-bonded water molecules are H-bonded with COO^-, a more obvious second peak, which is associated with the H-bonded O-O intermolecular stretching vibration, occurs at 290 cm^{-1}. Figure 10(b) presents the hydrogen spectrum, which is typically related to the libration (400–1200 cm^{-1}), intra-molecular bending (1200–2200 cm^{-1}), and intra-molecular stretching (2200–4000 cm^{-1}) motions. Table III presents the positions of the three main peaks for the hydrogen spectra of

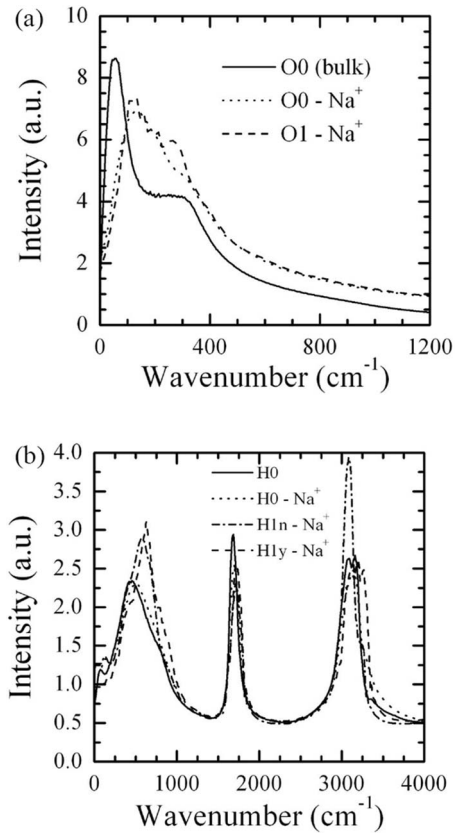

FIG. 10. Vibration spectra of (a) oxygen and (b) hydrogen atoms for the water molecules with the O atom bonded with Na^+ but in different interaction states with the COO^- groups. O0, O0-Na^+, and O1-Na^+ represent the O atoms in bulk water, in the water molecules bonded with Na^+, and in the water molecules simultaneously adsorbed to COO^- with one H atom and bonded with Na^+, respectively. Similar definitions apply to H atoms. In addition, H1y-Na^+, and H1n-Na^+ correspond to the hydrogen-bonded and non-hydrogen-bonded type of H atoms for the water molecules simultaneously adsorbed to COO^- with one H atom and bonded with Na^+.

each type of H atom in the water in more detail. In a comparison between H0 and H0-Na^+, the resultant hydrogen spectrum shifts slightly from a lower frequency for H0 towards a higher frequency for H0-Na^+. This is reasonable because the ion condensation is through the direct bonding with the O instead of the H atoms. When the Na^+-bonded water molecules are H-bonded with COO^-, the first two peaks of the

TABLE III. Positions of the three main peaks of hydrogen spectra for all the possible types of water molecules.

	Libration (cm^{-1})	Bending (cm^{-1})	Stretching (cm^{-1})
H0	462	1687	3160
H1n	524	1721	3052
H1y	762	1735	2984
H2	780	1782	2984
H0-Na^+	488	1696	3169
H1n-Na^+	577	1731	3080
H1y-Na^+	639	1731	3071
H0-Ca^{2+}	586	1749	3178
H1n-Ca^{2+}	612	1782	3092
H1y-Ca^{2+}	713	1786	3092

Downloaded 23 Apr 2012 to 140.112.148.95. Redistribution subject to AIP license or copyright; see http://jcp.aip.org/about/rights_and_permissions

resultant hydrogen spectra for both types of H atoms (H1n-Na^+ and H1y-Na^+) shift from a lower frequency for H0-Na^+ towards a higher frequency, whereas the third stretching peak shifts opposite. In addition, the shifting degrees of the three main peak positions from H0-Na^+ towards H1n-Na^+ and H1y-Na^+ are more significant than those obtained from H0 towards H0-Na^+. These results suggest a strong dependency of each type of H vibration mode in the water molecules, correlated to the formation of hydrogen bonds with the COO^- groups. It was observed when comparing the three peak positions of H2, H1y, H1n, and H0, as listed in Table III. When water molecules have stronger interactions with the COO^- groups through the formation of hydrogen bonds (H2 > H1y > H1n > H0), the resultant hydrogen spectra exhibit a larger increasing degree of the positions of the first two libration and bending peaks and a decreasing degree of the position of the third stretching peak.

Finally, we investigated how the dynamic properties of water molecules are influenced with an increase in the ionic bonding force. Parts (a) and (b) of Fig. 11 display the vibration spectra of oxygen (O0-Na^+ and O0-Ca^{2+}) and hydrogen (H0-Na^+ and H0-Ca^{2+}), respectively. As seen clearly, the stronger ionic bonds with Ca^{2+} make the resultant spectra of hydrogen and oxygen in the water to shift only slightly towards a higher wavenumber. A similar trend has also been observed when comparing the hydrogen vibration spectra of the two types of W1-Na^+, and W1-Ca^{2+} water molecules, as listed in Table III.

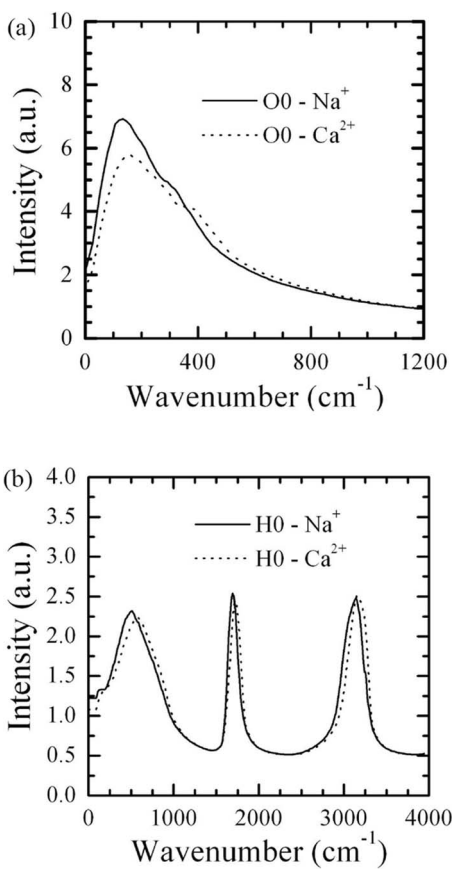

FIG. 11. Vibration spectra of (a) oxygen and (b) hydrogen atoms for the water molecules only bonded with Na^+ or Ca^{2+}. O0-Na^+, O0-Ca^{2+}, H0-Na^+, and H0-Ca^{2+} are different types of O and H atoms bonded with Na^+ and Ca^{2+}.

IV. CONCLUSIONS

We used all-atom molecular dynamics simulations to examine the condensation behavior of monovalent (Na^+) and multivalent (Ca^{2+}) salt counterions associated with the co-ions (Cl^-) surrounding the charged PMAA chain in water. The effects on the resultant chain conformation, the local arrangement, and the dynamic properties of water molecules in the highly diluted aqueous solutions were also investigated and discussed. We found that even when the salt ions are monovalent (Na^+), they tend to attract more than one COO^- group and act as a bridging agent within the polymer chain. The salt ions bridge between not only the "non-adjacent" but also the "adjacent" charged monomers, leading to a more coil-like and a locally stretched conformation, respectively. With an increase in the salt concentration, the amount of coiled-type condensed ions increase and reach a maximum. The numbers of stretched-type salt ions show an opposite trend and reach a minimum when the resultant chain conformation becomes the most collapsed. This result leads to the conclusion that the attractive interactions through the condensed salt ions between the non-adjacent monomers along the chain are responsible for the conformational collapse. When the salt concentration increases further into the expanded conformation regime, owing to the increased amount of Cl^- co-ions, we found a significant amount of the "stretched-type" condensed salt counterions outside surrounding the polymer chain. This is followed by the adsorption of the Cl^- co-ions and water molecules that tend to form a multilayer organization outside surrounding the PMAA chain. Thus, the expansion degree of the polyelectrolyte chain conformation becomes greatly limited.

Associated with the ion condensation, the most probable types of water molecules that exist within the polymer chain are water with one H atom bonded with the COO^- and water with the O atom bonded with the salt ion. Few water molecules are bonded simultaneously with two COO^- functional groups or with one condensed salt ion and one COO^-. When only the monovalent Na^+ ions are present in the solutions, water molecules are primarily adsorbed into either the condensed Na^+ ions or the COO^- groups. These adsorbed water molecules tend to form hydrogen bonds with each other and enhance the local bridging behavior associated with the condensation of monovalent Na^+ ions on the resultant chain conformation. When more multivalent Ca^{2+} salt ions are added, because Ca^{2+} provides a stronger attraction with COO^- or water, more water molecules are bonded directly to the condensed Ca^{2+} ions with only a few amount of water adsorbed into the condensed Na^+ ions. In this case, no bridging phenomenon through the water molecules was observed as in the condensation of Na^+. Instead, only the condensed Ca^{2+} ions provide a strong bridging effect within the polymer chain.

The strong attractive interaction between the salt ion and water via the formation of ionic bonds through the O atoms

Downloaded 23 Apr 2012 to 140.112.148.95. Redistribution subject to AIP license or copyright; see http://jcp.aip.org/about/rights_and_permissions

slows down the diffusion of water molecules. It causes a significant shift towards a higher frequency of the oxygen vibration spectrum with only a slight shift towards a higher frequency of the hydrogen spectrum for the water molecules. When the counterion-bonded water molecules are H-bonded with COO^-, the resultant oxygen spectrum shows a more obvious second peak that is primarily associated with the H-bonded O-O intermolecular stretching vibration. The formation of hydrogen bonds with the COO^- groups provides a stronger influence on the resultant hydrogen spectrum. In particular, it causes an increase in the positions of the first two libration and bending peaks and a decrease in the position of the third stretching peak.

ACKNOWLEDGMENTS

This work was supported by the National Science Council of Taiwan, Republic of China (Grant Nos. NSC-100-2628-E-002-020-MY3). The assistance of Dr. Saeed Doroudiani in editing the manuscript is gratefully acknowledged.

[1] *Handbook of Polyelectrolytes and Their Applications*, edited by S. K. Tripathy, J. Kumar, and H. S. Nalwa (Scientific, Stevenson Ranch, CA, 2002), Vol. 3.
[2] M. Delsanti, J. P. Dalbiez, O. Spalla, L. Belloni, and M. Drifford, ACS Symp. Ser. **548**, 381 (1994).
[3] M. Olvera de la Cruz, L. Belloni, M. Delsanti, J. P. Dalbiez, O. Spalla, and M. Drifford, J. Chem. Phys. **103**, 5781 (1995).
[4] J. Kötz, S. Kosmella, and T. Beitz, Prog. Polym. Sci. **26**, 1199 (2001).
[5] S. Hellebust, S. Nilsson, and A. M. Blokhus, Macromolecules **36**, 5372 (2003).
[6] P. Ravi, C. Wang, K. C. Tam, and L. H. Gan, Macromolecules **36**, 173 (2003).
[7] V. Sfica, and C. Tsitsilianis, Macromolecules **36**, 4983 (2003).
[8] C. Wang, P. Ravi, K. C. Tam, and L. H. Gan, J. Phys. Chem. B **108**, 1621 (2004).
[9] J. Yao, P. Ravi, K. C. Tam, and L. H. Gan, Polymer **45**, 2781 (2004).
[10] F. Muller, P. Guenoun, M. Delsanti, B, Demé, L. Auvray, J. Yang, and J. W. Mays, Eur. Phys. J. E **15**, 465 (2004).
[11] R. D. Wesley, C. A. Dreiss, T. Cosgrove, S. P. Armes, L. Thompson, F. L. Baines, and N. C. Billingham, Langmuir **21**, 4856 (2005).
[12] J. S. Jan and V. Breedveld, Macromolecules **41**, 6517 (2008).
[13] S. Block and C. A. Helm, Macromolecules **42**, 6733 (2009).
[14] Z. Luo and G. Zhang, Macromolecules **43**, 10038 (2010).
[15] Y. Roiter, O. Trotsenko, V. Tokarev, and S. Minko, J. Am. Chem. Soc. **132**, 13660 (2010).
[16] J. Wittner, A. Johner, and J. F. Joanny, J. Phys. II **5**, 635 (1995).
[17] P. Gonzalez-Mozuelos and M. Olvera de la Cruz, J. Chem. Phys. **103**, 3145 (1995).
[18] H. Schiessel and P. Pincus, Macromolecules **31**, 7953 (1998).
[19] N. V. Brilliantov, D. V. Kuznetsov, and R. Klein, Phys. Rev. Lett. **81**, 1433 (1998).
[20] T. T. Nguyen, I. Rouzina, and B. I. Shklovskii, J. Chem. Phys. **112**, 2562 (2000).
[21] F. J. Solis and M. Olvera de la Cruz, J. Chem. Phys. **112**, 2030 (2000).
[22] F. J. Solis and M. Olvera de la Cruz, Eur. Phys. J. E **4**, 143 (2001).
[23] F. J. Solis, J. Chem. Phys. **117**, 9009 (2002).
[24] P. Y. Hsiao and E. Luijten, Phys. Rev. Lett. **97**, 148301 (2006).
[25] P. Y. Hsiao, J. Chem. Phys. **124**, 044904 (2006).
[26] P. Y. Hsiao, Macromolecules **39**, 7125 (2006).
[27] A. Kundagrami and M. Muthukumar, J. Chem. Phys. **128**, 244901 (2008).
[28] M. J. Stevens and K. Kremer, J. Chem. Phys. **103**, 1669 (1995).
[29] M. J. Stevens and S. J. Plimpton, Eur. Phys. J. B **2**, 341 (1998).
[30] R. G. Winkler, M. Gold, and P. Reineker, Phys. Rev. Lett. **80**, 3731 (1998).
[31] R. Messina, C. Holm, and K. Kremer, J. Chem. Phys. **117**, 2947 (2002).
[32] R. G. Winkler, M. O. Steinhauser, and P. Reineker, Phys. Rev. E **66**, 021802 (2002).
[33] P. G. Khalatur, A. R. Khokhlov, D. A. Mologin, and P. Reineker, J. Chem. Phys. **119**, 1232 (2003).
[34] R. C. DeMille and V. Molinero, J. Chem. Phys. **131**, 034107 (2009).
[35] R. C. DeMille, T. E. Cheatham III, and V. Molinero, J. Phys. Chem. B **115**, 132 (2011).
[36] J. M. Y. Carrillo and A. V. Dobrynin, Macromolecules **44**, 5798 (2011).
[37] H. Morawetz and Y. Wang, Macromolecules **20**, 194 (1987).
[38] J. Zhang and N. A. Peppas, Macromolecules **33**, 102 (2000).
[39] S. V. Kazakov, V. I. Muronetz, M. B. Dainiak, V. A. Izumrudov, I. Y. Galaev, and B. Mattiasson, Macromol. Biosci. **1**, 157 (2001).
[40] S. P. Ju, W. J. Lee, C. I. Huang, W. Z. Cheng, and Y. T. Chung, J. Chem. Phys. **126**, 224901 (2007).
[41] M. J. Hwang, T. P. Stockfisch, and A. T. Hagler, J. Am. Chem. Soc. **116**, 2515 (1994).
[42] H. Sun, J. Phys. Chem. B **102**, 7338 (1998).
[43] J. M. Haile, *Molecular Dynamics Simulation* (Wiley, New York, 1992).
[44] D. C. Rapaport, *The Art of Molecular Dynamics Simulations* (Cambridge University Press, Cambridge, 1997).
[45] *The Basics of Theoretical and Computational Chemistry*, edited by B. M. Rode, T. S. Hofer, and M. D. Kugler (Wiley VCH, Berlin, 2007).
[46] *Inorganic Chemistry*, edited by P. Atkins, T. Overton, J. Rourke, M. Weller, and F. Armstrong (Oxford University Press, New York, 2010).
[47] G. E. Walrafen, M. S. Hokmabadi, W. H. Yang, and Y. C. Chu, J. Phys. Chem. **93**, 2909 (1989).
[48] J. A. Padro, J. Marti, and E. Guardia, J. Phys.: Condens. Matter **6**, 2283 (1994).
[49] J. Martí, J. A. Padro, and E. Guárdia, J. Chem. Phys. **105**, 639 (1996).
[50] A. Chandra, and T. Ichiye, J. Chem. Phys. **111**, 2701 (1999).
[51] N. Choudhury and B. M. Pettitt, J. Phys. Chem. B **109**, 6422 (2005).
[52] Z. Zhou, B. D. Todd, K. P. Travis, and R. J. Sadus, J. Chem. Phys. **123**, 054505 (2005).

Downloaded 23 Apr 2012 to 140.112.148.95. Redistribution subject to AIP license or copyright; see http://jcp.aip.org/about/rights_and_permissions